Científica, vol. 26, núm. 1, pp. 01-10, enero-junio 2022, ISSN 2594-2921, Instituto Politécnico Nacional MÉXICO
DOI: https://doi.org/10.46842/ipn.cien.v26n1a07

Truck Chassis Design and Analysis

Diseño y análisis del chasis para camiones

João Batista **De Aguiar**[1], José Manoel **De Aguiar**[2]

[1]Universidade Federal do ABC, BRASIL
https://orcid.org/0000-0002-1210-1242 | joao.aguiar@ufabc.edu.br
[2]Faculdade de Tecnologia de São Paulo, BRASIL
https://orcid.org/0000-0003-4371-3572 | josemaguiar@gmail.com2

Recibido 13-01-2022, aceptado 31-01-2022

Abstract
Commercial trucks of medium size are nowadays object of redesign of their structural system in the intent of increasing size or load capacity. The chassis is an essential element in this task. Many times, while keeping the front and rear overhangs of the chassis fixed, the inter-wheel distance is increased, sometimes with inclusion of an additional shaft, to allow that larger load containers with more capacity be used. Reconfigured geometrically, it has to support static and dynamic loads. In this sense a model of the ladder type chassis, post initial design, is submitted to alterations. Geometry, materials and loading are considered in a design method for hyperstatic conditions. Response of the model, using the finite element method, is presented to characterize diverse loadings. A set of critical sections is observed. Based upon the obtained results, the adequacy of the implemented method is verified.

Index terms: ladder chassis frame, modification, design, finite element analysis, results.

Resumen
Camiones comerciales de tamaño mediano suelen ser objeto de rediseño de su sistema estructural con el objetivo de aumentar tamaño o capacidad, el chasis es un elemento esencial en esta tarea. Muchas veces mientras se mantiene el tamaño de las partes delantera y trasera del chasis fijas, la distancia entre ejes es aumentada, incluso con la inclusión de eje adicional, para que contenedores mayores con más carga sean usados. Reconfigurado geométricamente el chasis debe soportar cargas estáticas y dinámicas. En ese sentido un modelo de chasis tipo escalera, posdiseño inicial, es sometido a alteraciones. La geometría, materiales y cargamento son considerados en uno método de diseño para condiciones hiperestáticas. La respuesta del modelo, utilizando el método del elemento finito, es presentada para su análisis en condiciones diversas de carga. Se observó un conjunto de secciones crítica y con base en los resultados obtenidos se realizó una adecuación de la solución propuesta.

Palabras clave: chasis tipo escalera, modificación, diseño, análisis por elemento finito, resultados.

I. INTRODUCTION

The chassis is the most important structural part of transportation vehicles, such as trucks. It holds the cabin, the container and its load. Its frame provides the points for the engine and gearbox, the suspension, the steering mechanism, power shaft, differential and axle assemblies as well as braking system [1]. It also holds compartments for accessories such as fuel, water and lubricant tanks, the kerb or empty weight. The chassis system is also a fundamental part of the resistance against impact, having to carry large loads in secure and stable conditions even in uneven roads. Its endurance has to be large to allow a large life in service.

Geometry of chassis systems is diverse. The ladder type frame is one of the oldest forms of chassis, being the mostly used, in part due to its versatility and reliability. These chassis are composed of two long channel beams held a part by a set of transverse elements. Design of the chassis takes into account flexural resistance in both planes – longitudinal and lateral - plus torsional resistance. Sizing may consider short, medium and large versions. In this last scenario, extension to comport longer load containers and or higher loads is sought, sometimes including the addition of an intermediate axle with concomitant extension of the chassis. Dimensioning and analysis in this situation is considered here.

Literature in chassis design includes diverse conditions. Chassis design and analysis for different combinations of cross sections [2] is one of the approaches. Optimization for weight reduction [3] is another. Finite element analysis is commonly used in these solutions.

II. HYPERSTATIC CHASSIS DESIGN

A design method for basic dimensioning of a chassis, set the arrangement, loading and chosen the material for the construction was presented previously [4]. From the procedure, profile and sectional modulae of the structural elements are determined, allowing the use of some fixed sections for the three versions of the chassis. Some restrictions have to be imposed in the process, as a maximum value of the load per wheel, maximum front and rear free spans, total length of the chassis as well as maximum traction per shaft may be ruled by authorities. In these circumstances, the chassis capacity is never plenty and another arrangement has to be considered. Normally inclusion of another shaft in the span between rear and front wheels is considered. The new shaft may be used for transmission or not. In this case the problem becomes hyperstatic to degree one. Use of additional shafts will increase the number of unknowns in the problem.

The original chassis is composed by the frame, with added suspension elements like parabolic and elliptic springs, dampers, water lubricant and fuel tanks, spare tires and supports to additional ware. Additionally, weight of engine, cabin and transmission elements is supported by the chassis frame. The empty weight K is the sum of these weight items. The payload is P. Total vehicle weight is then $W = P + K$. With additional overload allowance, upper load limit becomes $(1 + \eta)W$. In the design scenario, static conditions are supposed [5].

Having a chassis geometry set, let us considered what happens when an additional support is included with concomitant increase of length in such a way to keep the load per unit length fixed. As a pair of longitudinal beams carries the load, if uniformly distributed loading (UDL) is supposed, load on each beam is half of this value, Fig. 1. Therefore the load per unit length λ will be the ratio between $(1 + \eta)W/2$ and total length L, being the total length the sum of the front f, first inter-axis distance a, second inter-axis distance b, with the rear balance being r, $L = f + c + r$, $c = a + b$ [6]. We suppose the front and rear balances fixed.
Equilibrium equations in the $<X, Y>$ plane, Eq. (1), for the vertical efforts $<F, M, R>$, first, and moments about the Z axis, second, show a hyperstatic condition:

$$\begin{aligned} &F + M + R = \lambda L \\ &Ma + Rc = \lambda\left[rc + \frac{r^2}{2} + \frac{c^2}{2} - \frac{f^2}{2}\right] \end{aligned} \tag{1}$$

Inclusion of the relationship between the end moments $<M_{fm}, M_{mf}>$ and rotations $<\theta_f, \theta_m>$in the first inner spans of the chassis gives additional elements to unveil one of the unknown reactions above:

$$M_{fm} = 2EI[2\frac{\theta_f}{a} + \frac{\theta_m}{a}] - \frac{\lambda a^2}{12}$$
$$M_{mf} = 2EI[2\frac{\theta_m}{a} + \frac{\theta_f}{a}] + \frac{\lambda a^2}{12} \quad (2)$$

Analogous result may be written for the second inter-axis span:

$$M_{mr} = 2EI[2\frac{\theta_m}{b} + \frac{\theta_r}{b}] - \frac{\lambda b^2}{12}$$
$$M_{rm} = 2EI[2\frac{\theta_r}{b} + \frac{\theta_m}{b}] + \frac{\lambda b^2}{12} \quad (3)$$

Solution now requires compatibility conditions to be observed. In the front support, shear forcé $S_f = -\lambda f$ and bending momento $M_f = -\lambda f^2 / 2$ obey:

$$F + S_{f-} = S_{f+}$$
$$M_{fm} = M_{f-} \quad (4)$$

In the middle support, the shear forces at left, S_{m-} and at right, S_{m+} are related by the first equation below. Bending moments at these positions, $M_{m-} = -M_{mf}$ and $M_{m+} = M_{mr}$, are related according to the second one:

$$S_{m-} + M = S_{m+}$$
$$M_{mf} + M_{mr} = 0 \quad (5)$$

Finally, at the rear support, shear forces at left S_{r-} and at right, where $S_f = \lambda r$, may be related to the reaction R as in Eq. (6), first. Compatibility of bending moments around that support, with $M_{r+} = -\lambda r^2 / 2$ give the other:

$$R + S_{r-} = S_{r+}$$
$$M_{rm} = M_{r+} \quad (6)$$

The above set of compatibility equations may be introduced into the moment-rotation equations above, leading to the matrix-vector equation:

$$EI\begin{bmatrix} \frac{4}{a} & \frac{2}{a} & 0 \\ \frac{2}{a} & \frac{4}{a}+\frac{4}{b} & \frac{2}{b} \\ 0 & \frac{2}{b} & \frac{4}{b} \end{bmatrix} \begin{Bmatrix} \theta_f \\ \theta_m \\ \theta_r \end{Bmatrix} = \lambda \begin{Bmatrix} \frac{a^2}{12} - \frac{f^2}{2} \\ \frac{b^2}{12} - \frac{a^2}{12} \\ \frac{r^2}{2} - \frac{b^2}{12} \end{Bmatrix} \quad (7)$$

Solution of the system of equations, supposing a non-singular matrix, leads to the elements of the vector θ:

$$\theta_f = \frac{a}{12EIc}[(3c+b)\lambda_f - 2b\lambda_m + b\lambda_r]$$
$$\theta_m = \frac{ab}{6EIc}[-\lambda_f + 2\lambda_m - \lambda_r] \quad (8)$$
$$\theta_r = \frac{b}{12EIc}[a\lambda_f - 2a\lambda_m + (a+3c)\lambda_r]$$

Once the rotations above have been determined, introduction of the results into the pair of equations (2) and (3), lead to the end moments. The pair of bending moments in the first span allows determination of the shear force S_{f-} from equilibrium of bending moments:

$$S_{r-} = -\frac{1}{b}[M_{mr} + \frac{\lambda(r^2 + b^2)}{2}] \quad (9)$$

From the first of equations. (6), the reaction force R results. With this reaction, the pair of Eqs (1), will lead to the remaining reaction forces. The middle reaction writes as:

$$M = \frac{\lambda}{2a}[2rc + r^2 + c^2 - f^2] - \frac{Rc}{a} \tag{10}$$

being the other $F = \lambda L - R - M$.

The internal efforts in the first inter-axis span follows from the S_{f-} and M_{f-} as:

$$\begin{aligned} S(x) &= S_{f+} - \lambda x \\ M(x) &= M_{f+} + S_{f+}x - \frac{\lambda}{2}x^2 \end{aligned} \tag{11}$$

with distances x measured from the left support. Likewise, second inter-axis span may be written from shear force S_{m+}, bending moment M_{m+} and positions from left support x' in the form:

$$\begin{aligned} S(x') &= S_{m+} - \lambda x' \\ M(x') &= M_{m+} + S_{m+}x' - \frac{\lambda}{2}x'^2 \end{aligned} \tag{12}$$

Shear diagrams have linear stretches, while bending moments have parabolic distribution. The extreme values may be determined from the above expressions. Critical values $<S_c, M_c>$ will be used to find the maximum shear and flexural stresses. As area A and bending modulus W of the chassis parts are known – analysis problem - the mean shear stress $\tau_c = S_c / A$ and flexural stress $\sigma_c = M_c / W$ may be computed. The corresponding factor of safety will be

$$\iota_{<\sigma,\tau>} = \frac{< S_y, S_{sy} >}{< \sigma_c, \tau_c >},$$

being S_y and S_{sy} the yield strength – normal and shear - of the steel used in the chassis.

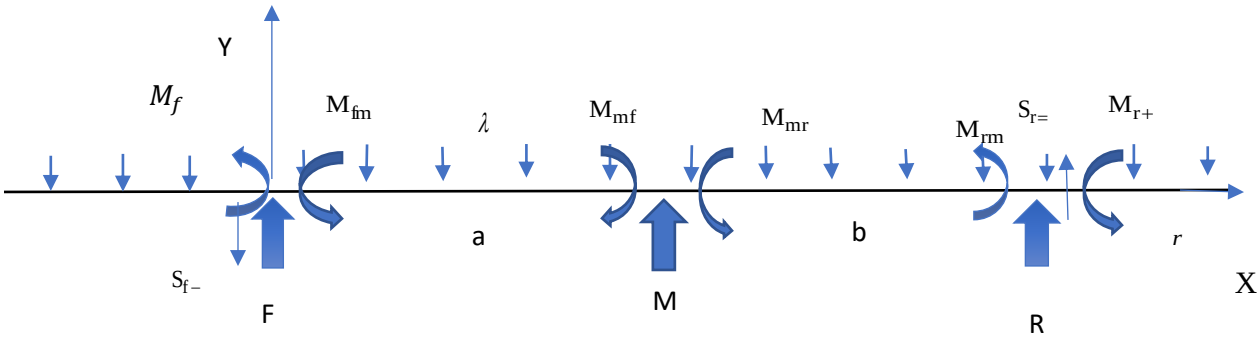

Fig. 1. Chassis beam on three supports.

III. CHASSIS ANALYSIS

In order to analyze the chassis, the finite element method, with allowance for non-linear effects is chosen. In it the stress field in a particular configuration may be obtained by formulating equilibrium with the principle of virtual work [7], that equates internal δW_i and external virtual work δW_e, where:

Científica, vol. 26, núm. 1, pp. 01-10, enero-junio 2022, ISSN 2594-2921, Instituto Politécnico Nacional MÉXICO
DOI: https://doi.org/10.46842/ipn.cien.v26n1a07

$$\delta W_i = \int_{V_t} \boldsymbol{\sigma} : \delta \boldsymbol{e}\, dV;$$
$$\delta W_e = \int_{V_t} \boldsymbol{b}.\delta \boldsymbol{d}\, dV + \int_{S_t} \boldsymbol{t}.\delta \boldsymbol{d}\, dS \tag{13}$$

being $\boldsymbol{\sigma} = \hat{\sigma}(\boldsymbol{x}, t)$ and $\boldsymbol{e} = \hat{e}(\boldsymbol{x}, t)$ the true stress and linear strains at the present configuration x at time t. Body forces $\boldsymbol{b}$ and tractions $\boldsymbol{t}$ at the present configuration work over virtual body and surface displacement fields to render the external work. Mapping the virtual work terms back to a known configuration $<S_0, V_0>$ transforms virtual work terms:

$$\delta W_i = \int_{V_0} \boldsymbol{S} : \delta \boldsymbol{\varepsilon}\, dV_0$$
$$\delta W_e = \int_{V_0} \boldsymbol{B}.\delta \boldsymbol{D}\, J_0 dV_0 + \int_{S_0} \boldsymbol{T}.\delta \boldsymbol{D}\, I_0 dS_0 \tag{14}$$

Where S and ε is a conjugate stress-strain pair – internal product, $\boldsymbol{B}$ and $\boldsymbol{T}$ - scalar product - are body and tractions obtained from the mapping into the previous configuration X_0. The displacement field is $\boldsymbol{D} = D(X_0)$; J_0 is the volumetric while I_0 is the surface area ratio. Upon introducing the interpolation of the virtual displacement field, $\boldsymbol{D} = \boldsymbol{N}\boldsymbol{D}^N$, being $\boldsymbol{N}$ the interpolation matrix, above expressions will turn into:

$$\delta W_i = \delta \boldsymbol{D}^N \int_{V_0} \ddot{\boldsymbol{B}} : \boldsymbol{S}\, dV_0$$
$$\delta W_e = \delta \boldsymbol{D}^N \int_{V_0} \boldsymbol{N}.\boldsymbol{B} J_0 dV_0 + \delta \boldsymbol{D}^N \int_{S_0} \boldsymbol{N}.\boldsymbol{T} I_0 dS_0 \tag{15}$$

whose difference will then be written as:

$$\delta W_i - \delta W_e = \delta \boldsymbol{D}^N \boldsymbol{\Psi} \tag{16}$$

The difference between internal and external generalized forces is null for equilibrium, so $\boldsymbol{\Psi} = \Psi(\boldsymbol{D}^N)$ becomes:

$$\boldsymbol{\Psi} = \int_{V_t} \overline{\boldsymbol{B}} : \boldsymbol{\sigma}\, dV - \boldsymbol{F}; \quad \boldsymbol{F} = \int_{V_t} \boldsymbol{N}.\boldsymbol{b} dV + \int_{S_t} \boldsymbol{N}.\boldsymbol{t} dS \tag{17}$$

with mapping back to present configuration. As the generalized forces vector depends on the displacement field $\boldsymbol{D}$, problem reduces to finding this vector field, which comprises the roots of the vector equation:

$$\Psi(\boldsymbol{D}) = \boldsymbol{0} \tag{18}$$

One way to obtain a solution to this sort of equation is by using Newton´s solution procedure. In order to apply it, the tangent matrix obtained from computing the increment of $\partial \boldsymbol{\Psi}$ in terms of the increment of displacement $\partial \boldsymbol{D}$ is needed. As the stress-displacement interpolation matrix consists of linear and non-linear parts, dependent upon displacements, component $\overline{B} = B_i + B_{nl}$, leads to:

$$\partial \Psi = \int_{V_0} (\partial B_l + \partial B_{nl}).\boldsymbol{S} dV_0 + \int_{V_0} (\boldsymbol{B}_l + B_{nl}).\partial S dV_0 \tag{19}$$

Assuming stresses and strains related by the constitutive relation:

$$\partial \boldsymbol{S} = \boldsymbol{C}_T : \partial \boldsymbol{\varepsilon}; \quad \partial \boldsymbol{\varepsilon} = (\boldsymbol{B}_l + \boldsymbol{B}_{nl}) \partial \boldsymbol{D} \tag{20}$$

Científica, vol. 26, núm. 1, pp. 01-10, enero-junio 2022, ISSN 2594-2921, Instituto Politécnico Nacional MÉXICO
DOI: https://doi.org/10.46842/ipn.cien.v26n1a07

It turns out that if the increment in Eq. (19) is written as $\partial \boldsymbol{\Psi} = \boldsymbol{K}_{\mathrm{T}} \partial \boldsymbol{D}^{\mathrm{N}}$, then:

$$\boldsymbol{K}_{\mathrm{T}} = \boldsymbol{K}_{\sigma} + \boldsymbol{K}_{\mathrm{l}} + \boldsymbol{K}_{\mathrm{nl}} \tag{21}$$

being the initial stress matrix given by:

$$\boldsymbol{K}_{\sigma} = \int_{\mathrm{V}_0} \partial \boldsymbol{B}_{\mathrm{nl}} . \boldsymbol{S} \mathrm{dV}_0 \tag{22}$$

and the normal linear stiffness matrix by:

$$\boldsymbol{K}_{\mathrm{l}} = \int_{\mathrm{V}_0} \boldsymbol{B}_{\mathrm{l}} . \boldsymbol{C}_{\mathrm{t}} \boldsymbol{B}_{\mathrm{l}} \mathrm{dV}_0 \tag{23}$$

Finally, the non-linear, or large displacement stiffness matrix will be:

$$\boldsymbol{K}_{nl} = \int_{V_0} \boldsymbol{B}_{l} . \boldsymbol{C}_{t} \boldsymbol{B}_{nl} dV_0 + \int_{V_0} B_{nl} . \boldsymbol{C}_{t} \boldsymbol{B}_{l} dV_0 + \int_{V_0} \boldsymbol{B}_{nl} . \boldsymbol{C}_{t} \boldsymbol{B}_{nl} dV_0 \tag{24}$$

These results may be mapped back to the present configuration.

Equilibrium, Eq. (18), may be attained using Newton-Raphson procedure [8]. In that, at some iteration point, $\boldsymbol{\Psi}(\boldsymbol{D}_{\mathrm{i}}) \neq \boldsymbol{0}$, making $\boldsymbol{\Psi}(\boldsymbol{D}_{\mathrm{i}}) + \partial \boldsymbol{\Psi} = \boldsymbol{0}$, where $\partial \boldsymbol{\Psi} = \boldsymbol{K}_{\mathrm{T}} \partial \boldsymbol{D}$, results in:

$$\partial \boldsymbol{D} = -\boldsymbol{K}_{\mathrm{T}}{}^{-1} \boldsymbol{\Psi}(\boldsymbol{D}_{\boldsymbol{i}}) \tag{25}$$

Stress field obtained in this analysis, is relative to a static, or pseudo static loading. Resulting equations for the discretized geometry are solved with the processor of program Abaqus™ [9].

IV. RESULTS

The basic chassis for a short/medium/large version has channel profile of height H, width B and thickness T with values <250, 80, 7> mm, and sectional modulus $W = 1.48e\text{-}4$ m^3 for lengths ranging from 7 up to 9 m [4]. The transversal tubular elements have circular section of diameter $D_t = 0.20$ m with thickness of 5 mm. These elements are disposed at regular distance from each other. The width of chassis is in the $0.90 < W < 1.00$ m range.

In the extended hyperstatic model, values of bending moment show that the critical value occurs at the rear shaft with value $M_c = -41.773e + 3\ N$ m. Supposing the material used in the construction of the chassis has the properties presented in Table 1, with yield resistance $S_y = 345$ MPa, shows that the flexural stresses are $\sigma_{rc} = M_c / W = 281.6$ MPa, giving a safety factor, for nominal load, equal to 1.22.

TABLE 1
MATERIAL PROPERTIES

Mechanical Properties	Value
Elastic Modulus E GPa	307
Poisson's ratio ν	0.33
Mass density ρ kgm	7.87e+0
Yield Strength S_{yt} MPa	345
Ultimate Strength S_{ut} MPa	460

Científica, vol. 26, núm. 1, pp. 01-10, enero-junio 2022, ISSN 2594-2921, Instituto Politécnico Nacional MÉXICO
DOI: https://doi.org/10.46842/ipn.cien.v26n1a07

A. Uniformly distributed load (UDL)

In order to obtain the response of the chassis frame to loading, a finite element model using shell elements is constructed. The model consists of a pair of longitudinal channel beams of length l = 12 m, with front overhang f = 1.5 m, inter-wheel distance $c = a + b$ = 8 m and rear overhang r = 2.5 m, connected by a set of eleven tubulars of length w = 1 m each, enclosed by front and rear channels. Total load in this configuration is W = 27 tonf. Figure 2 shows the discretized model of the chassis under uniform load distribution, in static condition, being supported in front, middle and rear.

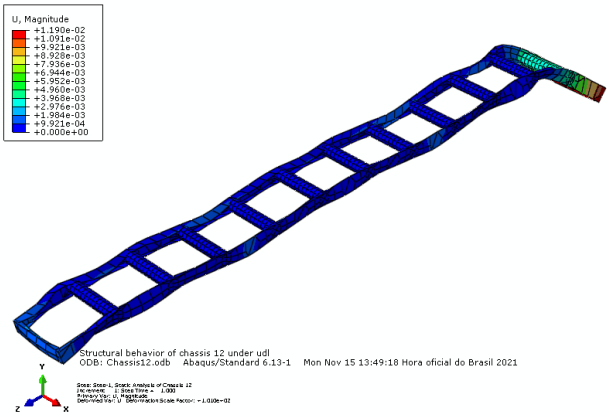

Fig. 2. Finite element model of chassis.

The chassis has in the front part a pair of parabolic springs, 1 m a part, placed symmetrically around the front wheels. In the middle and rear, a pair of elliptic springs under same distance, symmetrically disposed, around middle and rear shafts is used. Under the action of the uniformly distributed loading, inelastic phenomenae do not take place in the chassis, as Figure 3 shows for Mises stresses. Torsion in the frame is quite small for this loading.

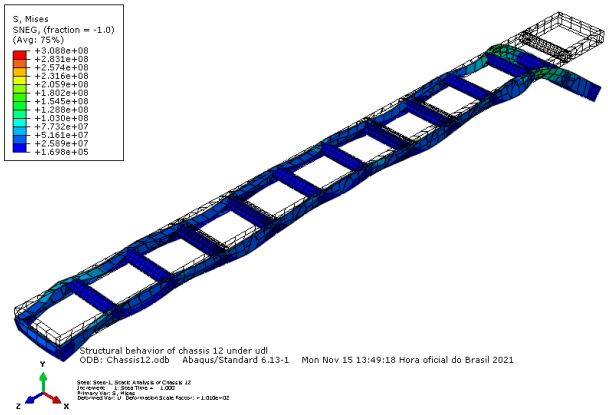

Fig. 3. Mises stress contour for hyperstatic chassis.

B. Applied wheel displacement

While loaded in transport situations, uneven pavement conditions are frequently encountered. In Fig. 4 this case is considered with application of an applied displacement to the suspension system at the front left wheel corresponding to 2.5 tonf. This condition entails appearance of torsional effects. Even though the design scenario did not contemplate these conditions, maximum stresses occurring in the chassis did not show much higher values. Equivalent elastic stresses were less than the yield resistance of the material, $\sigma' < S_{yt}$ all over. However, inelastic instability appeared in the webs of some channel sections. In order to mitigate these effect vertical struts, have to be installed in the space between webs to divide the free span and make this occurrence less possible – detailing process. Initial instability analysis, buckling, is a perturbation method applied around the initial unloaded configuration. Instability may be verified considering the increment vector $d\boldsymbol{\Psi}$ referred to a stable initial linear condition $\boldsymbol{K}_{n1} = 0$, so that $\partial\boldsymbol{\Psi} = 0$. Increasing the loads by a factor λ, we look for a value of this parameter such that

$$\partial\boldsymbol{\Psi} = (\boldsymbol{K}_1 + \lambda\boldsymbol{K}_\sigma)\partial\boldsymbol{D} = \boldsymbol{0} \tag{26}$$

This requires the determinant of the stiffness matrix be null $\det[K_1 + \lambda K_\sigma] = 0$. Obtained values of λ are the eigenloads that cause instability. Buckling load multipliers for original chassis are shown in Table 2. In general buckling takes place around the rear axle. Each mode has a particular geometry indicating different forms of buckling according to the order of appearance of them. Local and global forms occur in the sequence.

TABLE 2. INSTABILITY LOADS OF CHASSIS.

Buckling Mode	Eigenvalue
1	3.2981
2	3.3379
3	-3.5911
4	3.5920
5	3.6208

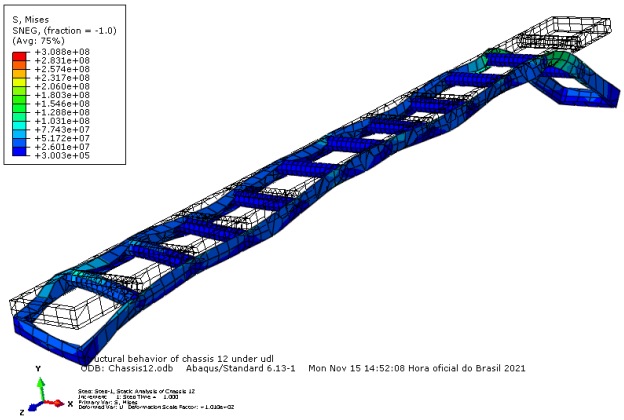

Fig. 4. Mises stress field for a front wheel vertical displacement.

Científica, vol. 26, núm. 1, pp. 01-10, enero-junio 2022, ISSN 2594-2921, Instituto Politécnico Nacional MÉXICO
DOI: https://doi.org/10.46842/ipn.cien.v26n1a07

C. Axial inertial force

Presence of motion, with traction loading appearing in the wheels, brings inertial loads in the axial direction of the chassis. For one g acceleration, the obtained reactions are shown in Fig. 5, with a multiplier of 10. Induced normal efforts will bring an additional degree of hyperstaticity to the problem.

Another factor of concern is the association between working frequency range of the engine installed in the truck and the natural frequency of the chassis. In general, trucks have engines of large power, capable of large tractions; working at low velocities, say in the 1000-2000 rot/min, or 16.5 – 33.3 rot/sec [10]. These excitations should be well off the range of the natural frequencies of the chassis in order to avoid resonance. Determination of the natural frequencies and associated mode shapes of the chassis comes from the solution of the problem:

$$(K_l - \omega_i^2 M)D_i = \mathbf{0} \tag{27}$$

For the set of frequencies ω_i and associated modes $\boldsymbol{D}_i$ that make Eq. (27) null, when neither the first term, in brackets, nor the second, are null. In this case, first five frequencies were requested, with values well off the working frequency range of the normal engines.

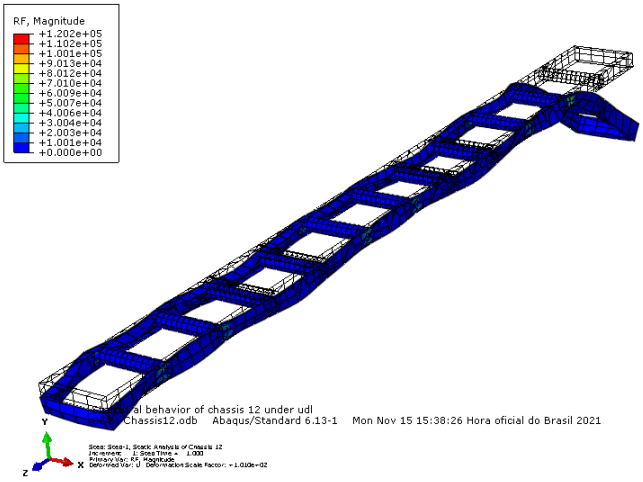

Fig. 5. Reaction efforts when inertial forces are present.

V. CONCLUSIONS

Results show that modifications in chassis configurations can attend the requisites initially proposed. The initial design was conceived to guarantee certain flexibility for increments in load and size at the expense of weight. Also the design method for hyperstatic cases shows good agreements when UDL conditions are used in finite element analysis. Instability analysis, on the other hand, showed that buckling would occur if preventive measures, like installation of vertical struts in the middle of the span of sequential tubulars weren´t taken. Critical section is usually at the rear shaft, where reinforcements should be provided after second order local analysis. The larger deflections in the UDL condition occurred in the end of the rear overhang under the acceptable range.

Científica, vol. 26, núm. 1, pp. 01-10, enero-junio 2022, ISSN 2594-2921, Instituto Politécnico Nacional MÉXICO
DOI: https://doi.org/10.46842/ipn.cien.v26n1a07

REFERENCES

[1] A. S. Patel, J. Chotransh, "Design and analysis of TATA 2518TC truck chassis frame with various cross sections using CAE tolls," *International Journal of Engineering Sciences and Research Technology*, vol. 5, issue 9, pp. 692-714, 2016.
[2] M. S. Agrawal, "Design and Analysis of Truck Chassis Frame," *IOSR Journal of Mechanical and Civil Engineering*, pp. 76-85, 2018.
[3] C. Ramesh, A. Kulshreshtha, "Chassis Stress Analysis and Optimization by using ANSYS," *IJSRD International Journal for Scientific Research and Development*, vol. 3, issue 8, pp. 8-13, 2015.
[4] J. B. De Aguiar, J.M. De Aguiar., "Static Design and Analysis of a Truck Chassis," *XX Congreso Nacional de Ingenieria Eletromecânica y de Sistemas*, CNIES 2021, México, Nov. 2021.
[5] M. S. Agrawal, Md. Razik, "A Review on Study of Analysis of Chassis," *International Journal of Modern Engineering Research*, vol. 3, issue 2, pp. 1135-1138, 2013.
[6] V. K. Mulakalapalli, I. R. K. Raju, "Strength Evaluation of Tipper Chassis under Static and Dynamic Load Conditions," *International Research Journal of Engineering and Technology*, vol. 5, issue 11, pp. 1716–1728, 2018.
[7] O. C. Zienckiewicz, R. L. Taylor, J.Z. Zhu, *The Finite Element Method: Its Basis and Fundamentals*, Butherworth-Heinemann, 7th ed., 2013.
[8] K.J. Bathe, "Finite Element Procedures in Engineering Analysis," Prentice-Hall, 2nd ed., 2006.
[9] Abaqus Simulia 6-13-1, Abaqus Inc., Dassault Systèmes, 2013.
[10] R.G. Budynas, J.K. Nisbett, *Shigley´s Mechanical Engineering Design*, McGraw-Hill, 10th ed., 2015.

Científica, vol. 26, núm. 1, pp. 01-10, enero-junio 2022, ISSN 2594-2921, Instituto Politécnico Nacional MÉXICO
DOI: https://doi.org/10.46842/ipn.cien.v26n1a07